Eco. Env. & Cons. 30 (August Suppl. Issue) : 2024; pp. (S97-S107)
Copyright@ EM International
ISSN 0971–765X

DOI No.: http://doi.org/10.53550/EEC.2024.v30i05s.016

Efficacy of Okra pod extracts as a natural polymeric flocculant for kaolin suspension

Tanbir Nasim

Department of Chemistry, Bijoy Krishna Girl' College, University of Calcutta
Address: 5/3, M.G. Road, Howrah 711 101, W.B., India

(Received 29 January, 2024; Accepted 28 March, 2024)

ABSTRACT

This is probably the first report on flocculation of kaolin suspension using Okra pod extract (OP) as a novel biflocculant, which is very cheap and can be readily obtained. The flocculation experiments are done with OP at various pH and using different concentrations of OP. Settling time and turbidity were measured to optimize flocculant dose and pH. The flocculation experiments show that the optimum flocculant dose for kaolin suspension is 25 ppm, whereas 2.6 is the optimum pH. Reduced viscosity, average molecular size, zeta potential of the flocculants are measured, and scanning electron microscope images and water entrapment values of the resultant flocs are done to understand the mechanism of the flocculation process. Fourier transformed infrared, Nuclear magnetic resonance analysis and gel permeation chromatography have been performed on OP extracts to understand the content of the extract.

Key words: *Okra pod extract, Kaolin, Flocculant, Turbidity, Zeta potential*

Introduction

The global population will increase by 40% to 50% in the next fifty years. The growing population, ceaseless industrialization and increasing urbanization all over the world have been leading to severe water crisis all over the world. The fresh water content of the world is also depleting very fast. Consequently, the treatment of the waste water form household, agriculture and industry becomes quite essential to deal with ever increasing demand for water. One of the most convenient and widely used methods for water treatment is flocculation (Koohestanian *et al.,* 2008). The flocculation can be achieved by inorganic flocculants or polymeric based organic polymer. Use of inorganic flocculants (Gao *et al.*, 2005; Liu *et al.,* 2012) is becoming a rarity due to the following reasons- (a) high flocculant dosage of inorganic flocculants is required, (b) severe toxicity of the metal ions causes the treated water harmful, (c) these flocculants produce large amount of sludge, so it becomes difficult to deal with afterwards and (d) operation cost is very high, as it requires high flocculant dose. But, polymeric flocculants are generally superior over inorganic flocculants because of their low flocculant dose, lesser sludge content and they are less expensive than the inorganic flocculants. Poly (acryl amide) and its derivative have been used as flocculant widely all over the word, but their popularity is diminishing because the presence of toxic monomer in their sample as impurity (Besra *et al.,* 2006). In this scenario, instead of using synthetic polymeric flocculant, the flocculation efficacy of naturally occurring polymeric material such as starch, chitosan, guar gum, glycogen, dextrin etc has been observed and the results are quite promising (Bratskaya *et al.,* 2005; Nasim *et al.,* 2013). The natural polymeric

flocculants are superior over synthetic ones as they are biodegradability and they do not contain any toxic monomers in their sample. Nowadays, scientists are giving more attention on the natural materials (Hamid *et al*., 2016; Xie *et al*., 2007) which can be used either in raw form or after little pre-treatment, therefore, the operational cost becomes quite lesser in comparison to the other flocculants used. As the flocculants can be extracted easily from the local trees, so it provides an eco-friendly localised treatment of water, which can be used by common people with very minimal technical apparatus. The extracts from the *Moringa oleifera, Nirmali seeds, cactus, tannin, Acacia nilotica* tree etc are successfully used for waste water treatment as bioflocculants (Miller *et al*., 2008; Nasim *et al*., 2018).

Kaolin is used in cement, paint, pigment, paper filler, ceramics etc industries (Faqir *et al.,* 2017). So, the global demand of kaolin is very huge. These industries face a problem of separating kaolin particles form its water effluents as kaolin forms a stable suspension due to very colloidal size, anisotropic shape and negatively charged basal faces (McFarlane *et al.,* 2005). Because of the above-mentioned reasons, the small kaolin particles do not coalesce to form large agglomerates and so it produces stable suspension. The bioflocculants bind with number of kaolin particles forming a larger floc (bridging mechanism) or they can neutralise the negative charge on the surfaces of the particles which eventually minimize the repulsions among the kaolin particles so they can come closer to form agglomerates (Nasim *et al*., 2014). These flocs then settle down by the force of gravity.

In this investigation, a thorough study has been carried out to observe the flocculation efficiency of okra pod extracts to remove kaolin particles from this suspension. The flocculation efficacy was determined by measuring the settling time and residual turbidity of the suspension after mixing the required dose of flocculant. The flocculation experiments are carried out at different pH using various amount of flocculant dose to optimize the best flocculation condition for kaolin suspension. Fourier transformed infrared, Nuclear magnetic resonance analysis and gel permeation chromatography have been performed on OP extracts to understand the nature of the extract. Ferric chloride, calcium chloride and sodium chloride are mixed in settling cylinder to aggravate the flocculation potential of OP. It is found out that calcium chloride shows better results in comparison to ferric chloride and sodium chloride

Experimental

Materials

Kaolin (suspension zeta potential"4.9 mV at pH 7) was purchased from B.D. Pharmaceuticals Works Pvt. Ltd, Howrah, West Bengal, India. Okra was collected from the local market in West Bengal. NaCl, $CaCl_2$ and $FeCl_3$ were purchased from Loba Chem, Mumbai, India. Tap water, used for flocculation study, had the following specifications: pH 7.0–7.3, turbidity H" 0.1 NTU, total hardness equal to12 mg $CaCO_3$ per litre. Other reagents like solid sodium hydroxide beads, concentrated hydrochloric acid, Anthrone and 3,5-dinitro salicylic acid, all of laboratory grades were obtained from indigenous sources.

Characterization of OP extracts

Estimation of total sugar and reducing sugar in OP extracts

The total sugar content in the OP extract was estimated by using Anthrone method. In brief, 1 ml of the sample solution (1mg/ml) was taken in a test tube and mixed with 4 ml of freshly prepared Anthrone. The mixture was subsequently boiled in water bath at 100 °C for 10 min and then was allowed to cool down to the room temperature (25 °C). The optical density was measured at 620 nm by using a UV spectrophotometer (Agilent Carry 100). The concentration of total sugar in the sample was calculated by using a calibration curve made from standard glucose solutions.

Reducing sugar content in the sample was determined by using 3, 5-dinitrosalicyclic acid (DNSA) method. 1 ml of the sample solution (1mg/ml) was taken in a test tube, to that 3 ml of DNSA was added. The mixture was boiled at 100 °C for 15 min to develop brick red colour. It was then allowed to cool down for colour stabilization. The absorbance was recorded at 575 nm by using the same UV spectrophotometer. The concentration of total reducing sugar in the sample was calculated by using calibration curve made from standard glucose solutions.

Fourier transformed infrared spectroscopy (FTIR) analysis

Fourier transformed infrared (FTIR) spectral analysis of the samples were done in a JASCO FTIR spectrophotometer within the spectral range of 400 cm^{-1}

to 4000 cm^{-1} at a resolution of 4 cm^{-1} in dispersive mode. An average of 120 scans for each sample was reported for analysis.

Nuclear magnetic resonance (NMR) spectroscopy

The ^{1}H NMR spectroscopy was done in a spectrophotometer purchased from Bruker, Germany after re-dissolving the samples in D_2O. The spectral analysis was done at a 300 MHz applied field. The ^{13}C NMR spectrum was recorded in solid state using a spectrophotometer supplied by the same company. The applied field strength was 500 MHz.

Determination of average molecular weight and molecular weight distribution

Average molecular weight and molecular weight distribution of the natural materials was determined using a gel permeation chromatography (GPC) (Model: 2414; Make: Waters (I) Pvt. Ltd., USA). The mobile phase was in aqueous solution (HPLC grade water was used for that analysis). The solution of natural materials was filtered through Whatman syringe filter (0.45 μm) before it was injected into the column. The flow rate of the mobile phase was fixed at 0.6 ml/min, and the temperature of the column was kept at 30 °C during the analysis.

Flocculation study

The flocculation experiments were carried out with model waste water at room temperature. The waste water was prepared by dispersing 3 wt% kaolin. Required dose of flocculant solution was added to the suspension and the volume was made up to 100 ml in the graduated settling cylinder. The cylinder was further inverted 10 times for flocculant-kaolin homogeneous mixing. Finally, the change of interfacial height versus time data was collected until 25 cm from the initial height was diminished.

Turbidity analysis of the treated water

Turbidities of the supernatants after each experiment was measured at an interval of 1 hr using a Systronics Digital Nephelo-Turbidity Meter, Model 132, till that achieved a constant value. The measurement was carried out by comparing the experimental turbidities against a standard formazin suspension. In each case, 2 ml of the suspended liquid was withdrawn from the depth of 15 cm and the turbidity was measured. Initially the data was recorded for five hours with one hour interval and finally after 24 hr to observe any change in turbidity on prolonged standing.

Reduced viscosity study

Reduced viscosities of aqueous solutions of the flocculants and its blends at different pH were measured in an Ubbelohde Viscometer as per ASTM-D-445 (capillary no: II, ID: 1.13 mm) at room temperature (27^0C). The falling time (t) was measured at different concentrations. Relative (η_{rel}), specific (η_{sp}) and reduced viscosities (η_{red}) were calculated using the following formulae.

$\eta_{rel} = t/t_0$

$\eta_{sp=} \eta_{rel} - 1$

$\eta_{red} = \eta_{sp}/C$ …… (2.1)

Here, t_0 refers to the falling time of the solvent (water), C stands for concentration in g/dl.

Measurement of average molecular size and Zeta potential

Average molecular size of the flocculants and zeta potentials of both flocculants and the suspension at different pH were measured in a Dynamic Light Scattering instrument, Zetasizer nano-ZS90, purchased from Malvern, United Kingdom. In each case, the solutions were filtered using whatman no. 41 filter paper and the measurements were carried out with the filtrates.

Determination of Floc Size and size distribution

The floc size and size distribution (calculated using ImageJ basics; version 1.38 Software) were determined from the photomicrographs of the flocs taken under a scanning electron microscope (SEM, Carl Zeiss 5800). The machine was operated at an acceleration voltage of 15 KV. Dilute kaolin suspension of 0.9 wt% concentration was used for the study to avoid high collation effect. The finer flocs were captured during settling by using a long-handed spoon having its collecting site 90^0 apart from its holding site. The size distribution was calculated from the SEM images using ImageJ basics software; version 1.38.

Water Entrapment Calculation

Some fresh water is always removed during flocculation and thus it is important to calculate how much of the fresh water has been removed during each experiment. 1 g of the slurry after 24 hr of the experiment was taken and dried in a hot air oven for 1 hr at 110 ^{0}C. The weight difference obtained was expressed as the percentage water entrapped during

each experimentation.

Results and Discussion

Characterization of OP

Estimation of total sugar and reducing sugar content of OP

The total sugar content of OP estimated by Anthrone method is found to be 39.25% out of which 69.08% is the reducing sugar (estimated by DNSA method). Figure 1a-c shows the visuals of Anthrone experiment with OP (deep green colour denotes presence of sugar) and the respective calibration curves and experimental data used for estimation of the sugar content. Figure1d-f shows the corresponding images for DNSA test with OP (red colour denotes the presence of reducing sugar). The rest of the mass, i.e. 60.25% is thus the natural silica. The chemical reactions occurred during Anthrone and DNSA test methods have been demonstrated in Scheme 1 with glucose as a reference carbohydrate.

FTIR spectroscopic analysis

FTIR spectrum of OP is shown in Figure 2. It shows a broad transmission band in the region 3650-3050 cm^{-1} peak centred at 3395 cm^{-1}. It is attributed to vibration of hydrogen bonded O-H groups of the polysaccharide molecules. The weak transmittance at 2926 and 2856 cm^{-1} correspond to the characteristic anti-symmetric vibrations of C-H bonds both from CH and CH_2 units respectively. The peak at 1641 cm^{-1} arises due to the symmetric vibration of C-H unit. The transmission peak at 1730 cm^{-1} indicates the presence of –C=O group. The large number of peaks in the wave number region of 1450 to 1200 cm^{-1} is likely to be the complementary bending vibration of O-H and C-H bonds. Similarly, the peaks between 1186 and 953 cm^{-1} are due to bending vibration of C-O and C-C bonds of the polysaccharide molecules (Cao *et al.*, 2006; Hineno, 1977).

Analysis of ^{1}H and ^{13}C NMR spectrums of OP

Figure 3 displays the ^{1}H NMR spectrum of OP. It shows the resonances of H-2, H-3, H-4, H-5 and H-6 protons of the carbohydrate molecule between 3 and 4.5 ppm. Degeneracy in many of the peaks indicates similar other protons present in many other carbohydrate molecules. Plenty of resonance peaks indicates the presence of protons come from differ-

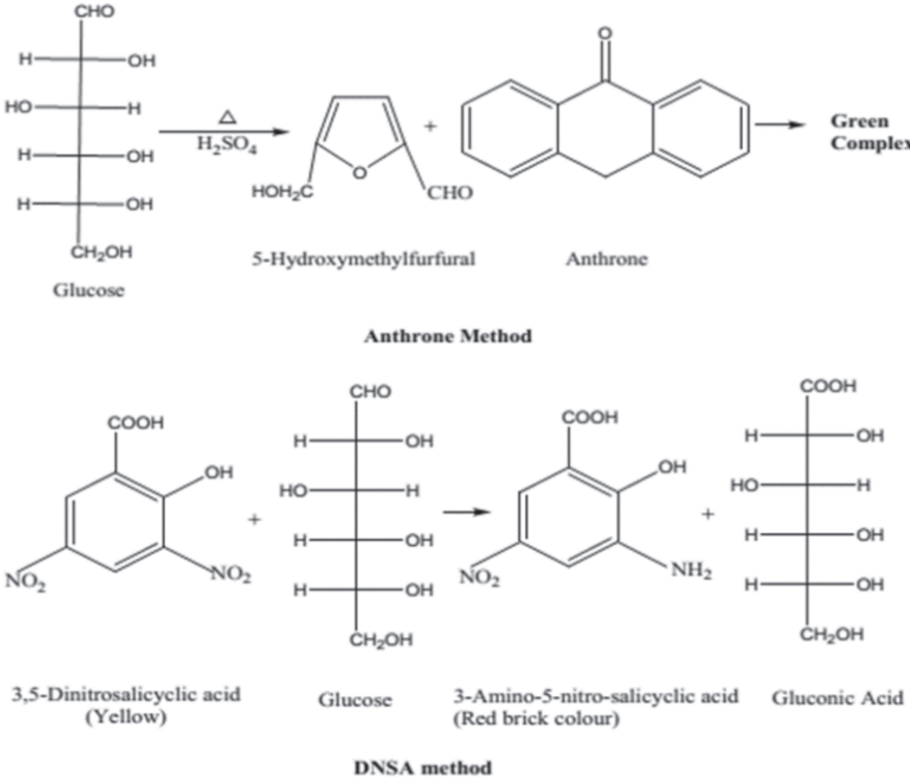

Scheme 1. Chemical reactions of Anthrone and DNSA methods respectively

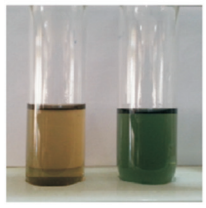

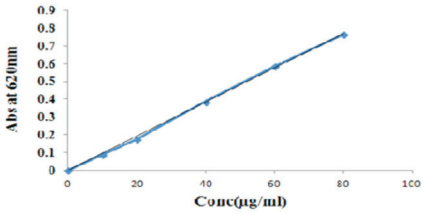

Conc. (µg/ml)	Abs. (620nm)	Conc. (µg/ml)	Final conc. (µg/ml)
0	0	0	
10	0.0872	9.083333	
20	0.1749	18.21875	
40	0.3876	40.375	
60	0.587	61.14583	
80	0.7654	79.72917	
Unknown	0.3768	39.25	1962.5

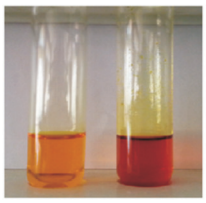

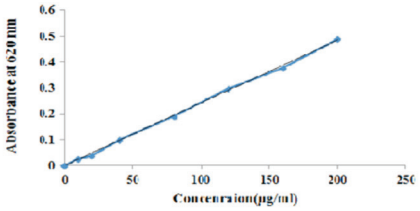

Conc. (µg/ml)	Abs (620nm)	Conc. (µg/ml)	Final conc.(µg/ml)
0	0		
10	0.026		
20	0.037		
40	0.099		
80	0.189		
120	0.299		
160	0.376		
200	0.489		
Unknown	0.1658	69.0833	345.4166

Fig. 1. Determination of sugar percentage through colourimetry: (a) positive Anthrone test showing the presence of carbohydrate molecule (A-blank, B-sample), (b) Standard calibration curve using glucose and (c) the experimental data on OP. Figure (d)-(f) show similar results on OP by DNSA method

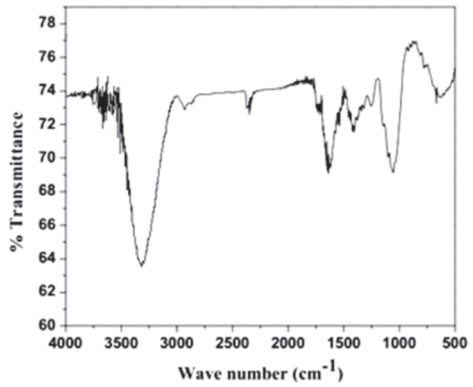

Fig. 2. FTIR spectrum of OP extract

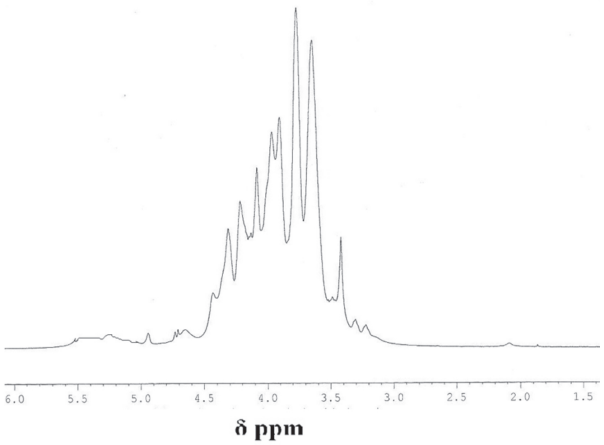

Fig. 3. ^{1}H NMR spectrum of OP

ent carbohydrate molecules. The anomeric proton H-1 shows the resonance at 4.9 ppm (Bagno *et al.*, 2007). Figure 4 shows the ^{13}C NMR spectrum of OP. It gives a evidence for the presence of carbohydrate in the micro-structure. The resonance peaks at 65, 71, 74, 77 and 81 ppm correspond to C-6, C-5, C-4, C-3 and C-2 carbons of the carbohydrate molecules respectively. The peak at 98 ppm is attributed to the anomeric carbon (C-1). There is another peak at 178 ppm which confirms the presence of carbonyl group in the micro-structure (Liu *et al.*, 2007).

Determination of molecular weight

Figure 5 shows the GPC chromatogram of OP. It measures both weight and number average molecu-

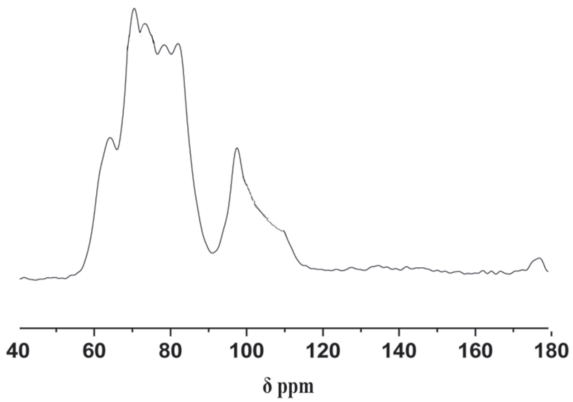

Fig. 4. ^{13}C NMR spectrum of OP

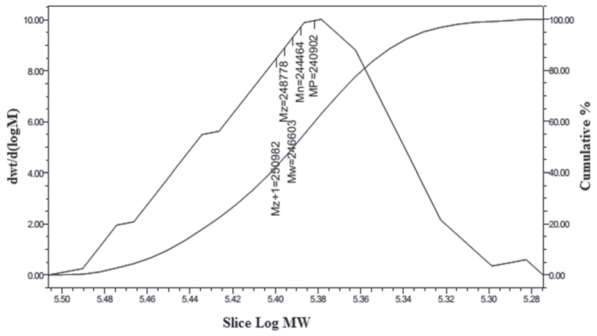

Fig. 5. GPC chromatogram of OP extract

lar weights of OP. The weight average molecular weight was 2.46×10^5 Da and the number average molecular weight was 2.44×10^5 Da with a PDI of 1.0087. Both high molecular weight and narrow PDI values are indicative of polysaccharide molecules as primary component of OP.

Effect of OP concentration on the flocculation of kaolin suspension

Flocculation experiments (with 3 wt% kaolin) suspension were carried out with different concentrations (9-35 ppm) of OP. Figure 6 compares the settling profiles. It takes 310.4 secs at 9 ppm for the suspension to lower the interfacial height, whereas it requires 275.14 and 236.43 secs in cases of 15 and 20 ppm respectively. 25 ppm OP takes the least time (193.68 secs). Beyond that the settling time increases to 359.76 secs using 35 ppm. Residual turbidities of the suspensions were also measured. The starting turbidity values in Figure 7 indicate the residual turbidity at each OP concentration. The lowest value of residual turbidity (15.6 NTU) was with 25 ppm,

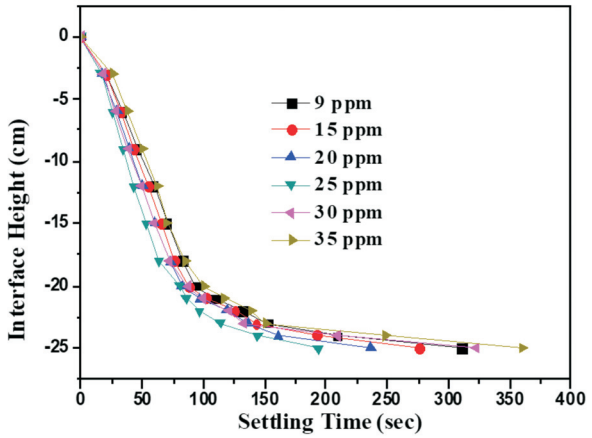

Fig. 6. Settling profiles of kaolin suspension using OP at different concentration

while both below and above this concentration, turbidities are higher which means the settling was not as efficient as obtained at 25 ppm. On standing the turbidity further drops for all the systems as recorded in Figure 7 and after 24 hrs shows much lower values, although the values are likely to decrease further on standing. Exponential drop in turbidity resembles second stage settling of the unsettled particles through the section of residual flocculant molecules. As expected, minimum turbidity of 4 NTU was obtained with 25 ppm dose after 24 hrs while the highest turbidity of 6.3 NTU was obtained with 35 ppm dose after equal interval.

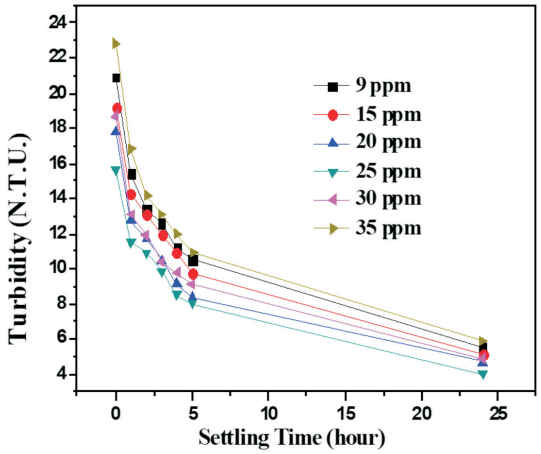

Fig. 7. Residual Turbidity analysis of kaolin suspension using OP of different concentrations for 24 hours.

The zeta potentials of both OP and kaolin are highly negative, thus, flocculation with OP through surface charge neutralisation pathway is possibly not a dominant factor. Instead interaction of various functional groups like –OH and –COOH with Si-OH groups of kaolin leading to adsorption over the clay particles is a feasible option for settling of the suspended particles. This is reflected from the zeta potential trend of OP at various concentrations. With increase in concentration starting from 9 ppm, the increasing numbers of both –OH and –COOH groups favours adsorption over the negatively charged kaolin surfaces overriding the repulsion interaction effect and this trend continues until 25 ppm concentration. But, beyond 25 ppm, a drastic increase in zeta potential causes repulsive interaction to dominate and prevent effective adsorption to occur. Measurement of zeta potential immediately after addition of OP in each case proved this hypothesis. Thus, optimization occurs at 25 ppm which

shows both the fastest settling and lowest turbidity at the end of the experiment. Hence, further optimization was carried out with 25 ppm dose.

Effect of pH on the flocculation efficacy of OP

Zeta potential and molecular size of flocculant molecules are susceptible to change with the change in pH of the medium. Hence, the flocculation efficacy of OP is verified under various conditions of pH c.a. 1.0, 2.0, 4.0, 7.0 and 10.0. As usual, when 25 ml 0.01% solutions of OP maintained at pH 1.0, 2.0, 4.0, 7.0 and 10.0 were added to the standard kaolin suspension and the volumes were made upto to 100 ml (i.e. 25 ppm), the pH of the suspension medium changed into 1.6, 2.6, 4.6, 7.0 and 9.4 respectively. Therefore, measurement of zeta potential, molecular size and reduced viscosity of OP were all carried out at the modified pH conditions for compliance. Figure 8 shows the settling profiles of kaolin at different pHIt is observed that the settling is faster in the strongly acidic region compared to the both basic and neutral regions It takes 135.02 and 116.1 secs at pH 1.6 and 2.6., whereas 172.57, 193.68 and 341.49 secs at pH 4.6, 7.0 and 9.4 respectively. So, there is a simple trend in settling rate of the OP at various pH, with the decrease in pH of the medium from pH 9.4, it takes normally lesser time to settle down the interface of the kaolin suspension. Thus, it is a homogeneous trend except for the fact that the settling is faster at pH 2.6 than at pH 1.6. Figure 9 demonstrates the residual turbidity values along with the long time turbidity analysis of suspensions. The residual turbidity values are well complied with the settling time data. $OP_{2.6}$ eventually produced maxi-

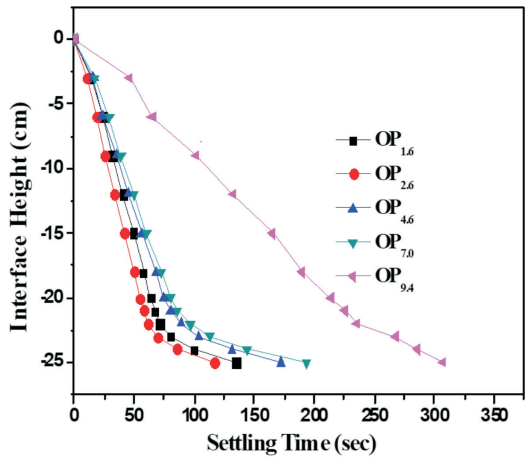

Fig. 8. Settling profiles of kaolin suspension using 25 ppm of OP at various pH

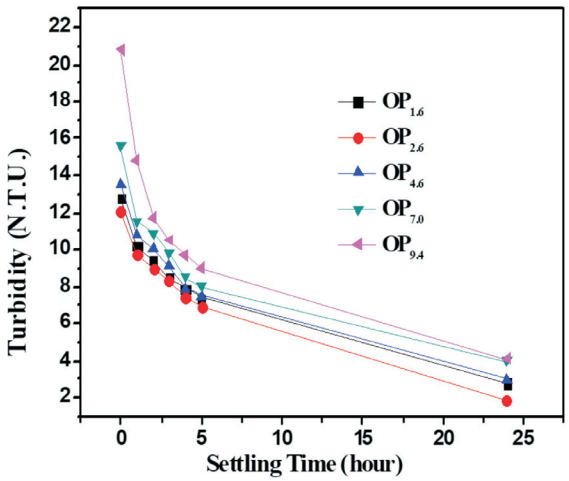

Fig. 9. Residual Turbidity analysis of kaolin suspension using 25 ppm OP at various pH for 24 hours

mum clarity at the end of the settling experiment (12.1 NTU). For other systems such as $OP_{1.6}$, $OP_{4.6}$, $OP_{7.0}$ and $OP_{9.4}$, the residual turbidities are 12.8, 13.6, 15.6 and 20.8 respectively. The results are well explained from zeta potential and molecular sizes of the OP. The zeta potential values at various pHs can be seen in Table 1. The potentials are slightly positive at pH 1.6 and 2.6 but at pH 4.6, it becomes negative and the values gradually increase along pH. At low pH both –OH and –COOH groups are protonated giving rise to a positive potential, however, at pH 4.6 only –COOH groups ionise due to very weak acidity and yield low negative value. But, at pH 7.0 and beyond both –COOH and –OH groups ionize to their conjugate bases and produce strong negative potential at higher pH. Figure 10 shows the molecular size distribution of OP at various pH. All along it shows a very narrow distribution and the average sizes bear unique correlation with zero potential values. The sizes actually reduced with increase in zeta potential value owing to intermolecular repulsion at this concentration excepting pH 2.6 where the average molecular size is higher than at pH 1.6. The molecular size data were further complemented from the reduced viscosities measured at different pH (Figure 11). Thus, it is now clear that the adsorption over kaolin was favoured at low zeta potentials and higher molecular sizes. Low zeta potential allows the molecules to come close enough to the clay particles for adsorption and longer molecular size favours interparticle bridging. Thus, both settling time and residual turbidity value were low when OP solution was made under high acidity such as

Table 1. Zeta potentials, net settling time, residual turbidity of kaolin suspension using OP

Sample	Flocculant Dose (ppm)	Modified pH	Zeta Potential (mV)	Net Settling Time (sec)	Residual turbidity (NTU)	Resultant Zeta Potential (after addition OP into Kaolin) (mV)
OP	9	7.0	-12.57	310.4	20.9	-6.99
OP	15	7.0	-13.43	275.14	19.2	-6.67
OP	20	7.0	-17.29	236.43	17.8	-5.76
OP	25	7.0	-22.78	193.68	15.6	-5.35
OP	30	7.0	-25.37	321.99	18.7	-7.09
OP	35	7.0	-26.74	359.76	22.8	-7.89
OP	25	1.6	+0.926	135.02	12.8	-1.04
OP	25	2.6	+0.192	116.1	12.1	-0.85
OP	25	4.6	-4.27	172.57	13.6	-4.49
OP	25	9.4	-32.43	307.41	20.8	-10.92

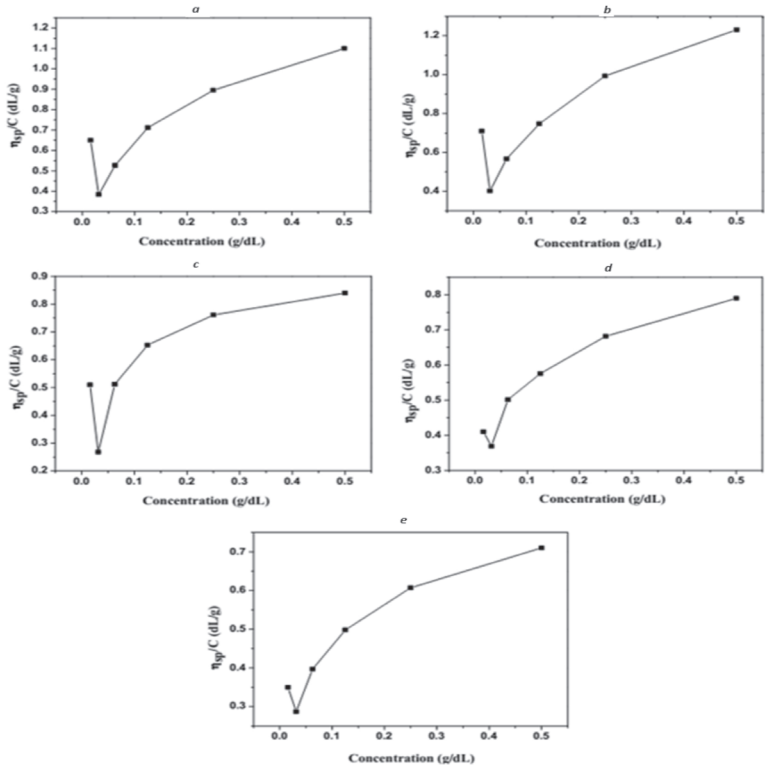

Fig. 10. Molecular size distribution of OP at pH (a) 1.6, (b) 2.6, (c) 4.6, (d) 7.0 and (e) 9.4.

pH 1.6 and 2.6. At pH 4.6, 7.0 and 9.4 both OP and kaolinhave strong negative potentials, which prevent the flocculant molecules to come in close proximity of the kaolin clay particles for both adsorption and interparticle bridging (although the bridging efficiency is thought to be poor at these conditions due to low molecular sizes). However, better performance of $OP_{2.6}$ over $OP_{1.6}$ is due to higher molecular size and lower zeta potential value. From the evidences achieved so far, it could be said that lower the value of the zeta potential, higher is the flocculation efficacy. $OP_{2.6}$ shows a potential of -0.85 mV and for $OP_{9.4}$, it is -10.92 mV and rest of the the least.systems come in between. Hence, $OP_{2.6}$ shown the highest efficiency while $OP_{9.4}$

Figure 12a-b demonstrates the SEM images of two representative cases at pH 2.6 and 9.4 respectively. The floc size datas are shown in bar diagrams alongside. It is quite clear from the figure that the flocs produced using $OP_{2.6}$ is larger in comparison to

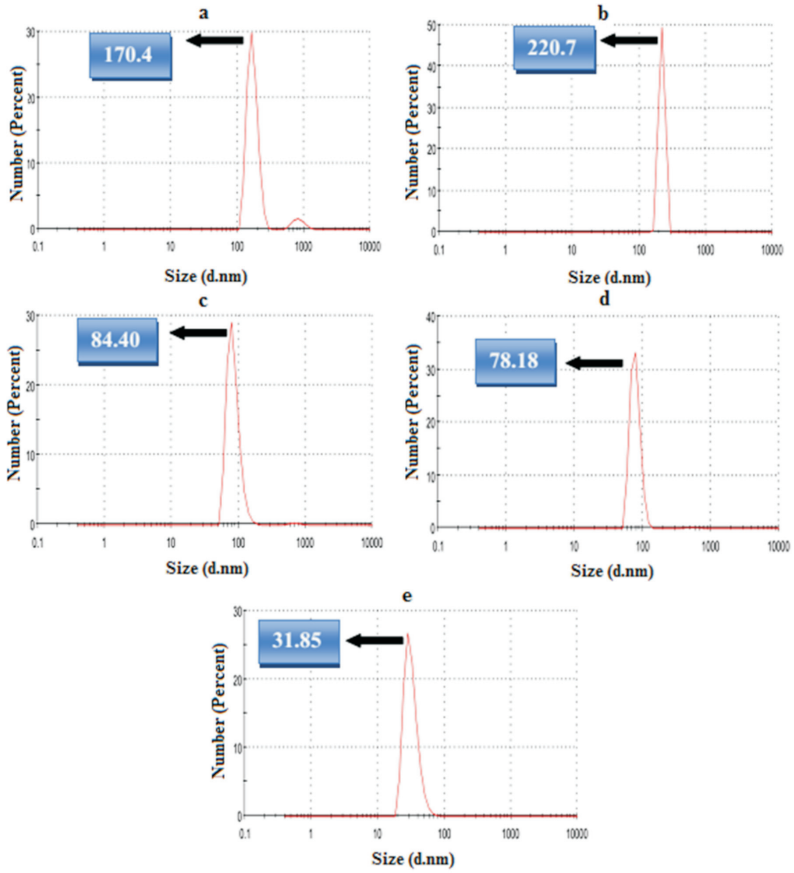

Fig. 11. Reduced viscosity vs concentration plot of OP at pH (a) 1.6, (b) 2.6, (c) 4.6, (d) 7.0 and (e) 9.4

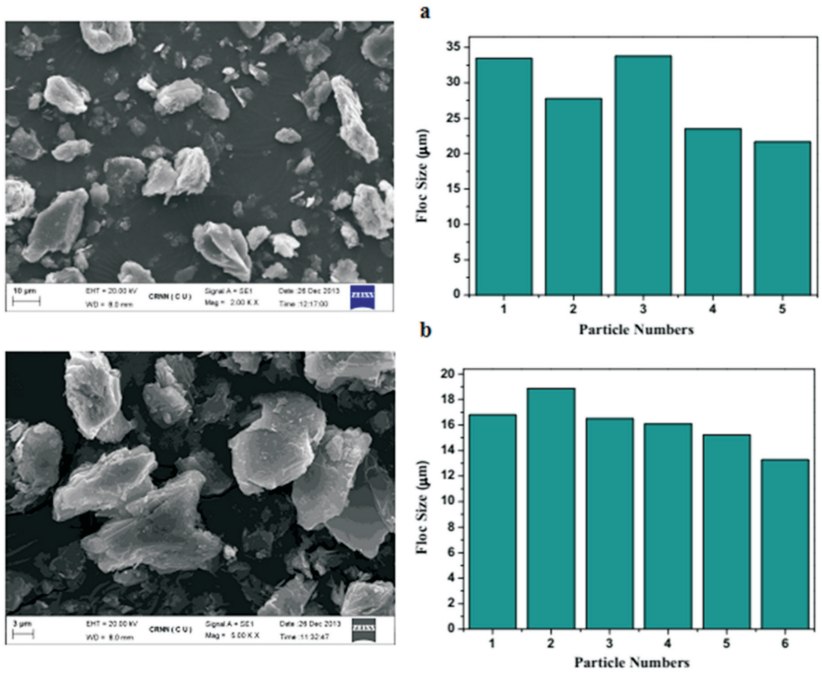

Fig. 12. SEM images of the flocs and its size distribution using OP at pH (a) 2.6 and (b) 9.4.

with $OP_{9.4.}$ Therefore, the floc density is less with $OP_{2.6}$ because they produced larger flocs. Larger flocs likely to possess more free space which favours the upward displacement of water faster from the bottom and eventually, reduces the overall settling time. Hence, $OP_{2.6}$ takes lesser time than $OP_{9.4}$ for settling. Higher floc size with more free space can simultaneously entrap excess amount of fresh water and can cause more fresh water loss. Figure 13 shows the percentage water entrapment in the flocs at different pH. $OP_{2.6}$ entrapped the maximum amount of fresh water (55.4%) in its sediment whereas $OP_{9.4}$ entrapped the least (46.1%). The water entrapment of $OP_{1.6}$, $OP_{4.6}$ and $OP_{7.0}$ were 52.1%, 48.3% and 46.8% respectively which were in compliance with their settling time data.

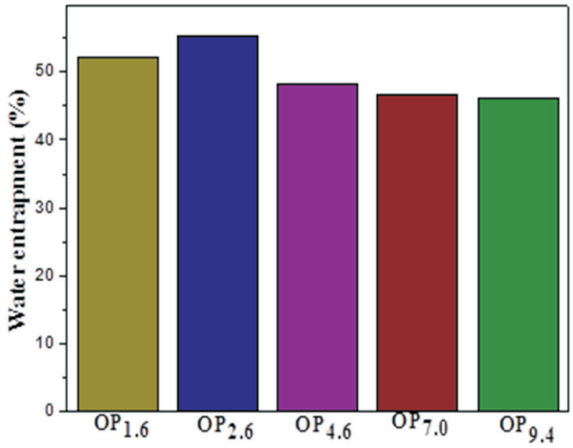

Fig. 13. Percentage of water entrapment in the flocs produced at various pH (a) 1.6, (b) 2.6, (c) 4.6, (d) 7.0 and (e) 9.4.

Effect of salts on the flocculation rate of $OP_{2.6}$

The effect of addition of monovalent sodium chloride (NaCl), divalent calcium chloride ($CaCl_2$) and trivalent ferric chloride ($FeCl_3$) on the flocculation efficacy $OP_{2.6}$ at different salt concentrations such as 0.01, 0.02, 0.03 and 0.04 M were examined. Figure 14 depicts the settling times in the presence of NaCl, $CaCl_2$ and $FeCl_3$ in the above- mentioned concentrations. It shows that NaCl actually enhances the settling time as the salt concentration is increased from 0.01 to 0.04 M. However, in cases of both $CaCl_2$ and $FeCl_3$, the settling time decreased for the first three concentrations levels i.e. 0.01, 0.02 and 0.03 M but increased at 0.04 M level. However, $CaCl_2$ has recorded greater reduction in settling time than $FeCl_3$. 0.03 M $CaCl_2$ reduced the settling time by nearly 7

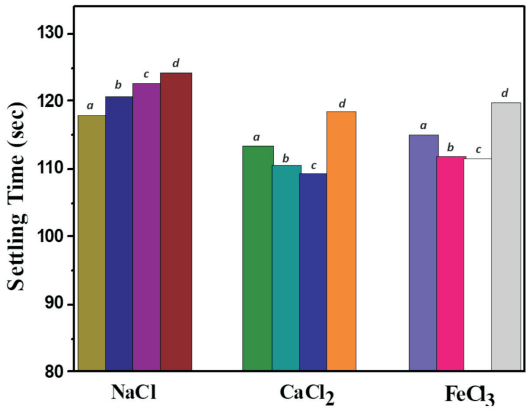

Fig. 14. Settling time profiles of kaolin suspension using $OP_{2.6}$ in presence of NaCl, $CaCl_2$ and $FeCl_3$ at (a) 0.01, (b) 0.02, (c) 0.03 and (d) 0.04 M concentrations

secs than $FeCl_3$. When either $CaCl_2$ or $FeCl_3$ was added to the suspension, the hydrolysed metal ions get adsorbed over the negatively charged kaolin particles. So, the repulsive interaction between the kaolin particles destabilized the suspension and thus when $OP_{2.6}$ was added to the suspension, it settled at a faster rate. But, beyond 0.03 M salt concentration the flocculation rate slowed down probably due to steric stabilization as observed in the previous chapter. The flocculant molecule was unable to come to the closest proximity of the colloidal particle to form bridges due to the presence of large number of hydrolysed metal ions on the colloidal surface. Because of high charge density of Fe^{3+} ion, the solvated size of the ions is higher than either Ca^{2+} or Na^{+}. As a consequence, Fe^{3+} showed poor result in comparison to Ca^{2+}. On the other hand, due to lowest charge density in the series, Na^{+} was unable to neutralize the surface charge of kaolin effectively instead had increased the concentration of positive charges on the surface which repelled the positively charged flocculant molecules and thus delayed the settling process.

Conclusion

It can finally be concluded that OP extract can act as efficient bioflocculant for kaolin suspension as it is cheap, easily available, eco-friendly and requires simple techniques. The optimum pH for OP extract is 2.6, whereas the 25 ppm dose is the optimum one. 0.04 M $CaCl_2$ can be added to kaolin suspension to increase the flocculation potential. As it is a natu-

rally occurring flocculant and can be bought from local market, it can be used in the household to treat their water without the assistance of any expensive apparatus.

Acknowledgement

The author wishes to acknowledge the authorities of Bijoy Krishna Girls' College and University of Calcutta for providing necessary support and essential technological facilities to carry out this work.

Conflict of Interest

There is no conflict of interest while preparing the manuscript.

References

Bagno, A., Rastrelli, F. and Saielli, G. 2007. Prediction of the ^{1}H-NMR and ^{13}C-NMR spectra of á-D-Glucose in water by DFT methods and MD simulations. *The Journal of Organic Chemistry*. 72 (19): 7373-7381.

Besra, L., Sengupta, D.K. and Roy, S.K. 2006. Influence of unadsorbed and weakly adsorbed flocculants on separation properties of kaolin suspension. *International Journal of Mineral Processing*. 78 (2):101-109.

Bratskaya, S., Schwarz, S., Liebert, T. and Heinze, T. 2005. Starch derivatives of high degree of functionalization: flocculation of kaolin dispersions. *Colloids and surfaces A: Physiochemical and Engineering Aspects.* 254 (1-3): 75-80.

Cao, W., Li, X.Q., Liu, L., Yang, T.H., Li, C., Fan, H.T., Jia, M., Lu, Z.G. and Mei, Q.B. 2006. Structure of an antitumor polysaccharide from *Angelica sinensis* (Oliv.) Diels. *Carbohydrate Polymers*. 66 (2): 149-159.

Faqir, N.M., Elkatatny, S., Mahmoud, M. and Shawabkeh, R. 2017. Fabrication of kaolin-based cement plug for CO_2 storage wells. *Applied Clay Science*. 141: 81-87.

Gao, Y., Wang, Y. and Yue, Q.Y. 2005. The chemical species distribution of aluminum in composite in composite flocculants prepared from Polyaluminum Chloride (PAC) and Polydimethyldiallylammonium Chloride (PDMDAAC). *Clean soil Air Water*. 33 (4): 365-371.

Hamid, S.H.A., Lananan, F., Khatoon, H., Jusoh, A. and Endut, A. 2016. A study of coagulating protein of *Moringa oleifera* in microalgae bio-flocculation. *International Biodeterioration and Biodegradation*. 113: 310-317.

Hineno, M. 1977. Infared spectra and normal vibration of β-D-glucopyranose. *Carbohydrate Research*. 56(2): 219-227.

Koohestanian, A., Hosseini, M. and Abbasian, Z. 2008. The separation method for removing of colloidal particles from raw water. *American-Eurasian Journal of Agricultural and Enironmental Sciences.* 4 (2): 266-273.

Liu, C., Lin, Q., Gao, Y., Ye, L., Xing, Y. and Xi, T. 2007. Characterization and antitumor activity of a polysaccharide from *Stronglycentrotusnudus* eggs. Carbohydrate polymers. 67 (3): 313-318.

Liu, X., Li, X.M., Yang, Q., Yue, X., Shen, T.T., Zheng, W., Luo, K., Sun, Y.H. and Zeng, G.M. 2012. Landfill leachate pretreatment by coagulation—flocculation process using iron-based coagulants: optimization by response surface methodology. *Chemical Engineering Journal.* 200-202: 39-51.

Mcfarlane, A. Bremmell, K. and Addai-Mensah, J. 2005.Microstructure, rheology and dewatering behaviour of smectite dispersions during orthokinetic flocculation. *Minerals Engineering.* 18 (12): 1173-1182.

Miller, S.M., Fugate, E.J., Craver, V.O. Smith, J.A. and Zimmerman, J.B. 2008. Toward understanding the efficacy and mechanism of *Opuntia* spp. As a natural coagulant for potential application in water treatment. *Environmental Science and Technology*. 42 (12): 4274-4279.

Nasim, T., Panda, A.B. and Bandyopadhyay, A. 2013. Guar gum and guar gum-oligomeric poly (vinyl alcohol) blends as novel flocculants for kaolinated waste water. *International Journal of Biological Macromolecules.* 58: 140-147.

Nasim, T., Pal, A. Giri, A., Goswami, L. and Bandyopadhyay, A. 2014. Exploring polyelectrolytic features of the exudate from native *Acacia nilotica* for flocculating aqueous kaolin suspension. *Separation and Purification Technology*. 131: 50-59.

Nasim, T., Pal, A. and Bandyopadhyay, A. 2018. Flocculation of aqueous kaolin suspension using a biodegradable novel flocculant system of poly (vinyl alcohol) and *Acacia nilotica* gum blends. *Applied Clay Science*. 152: 83-92.

Xie, C., Feng, Y., Cao, W., Xia, Y. and Lu, Z. 2007. Novel biodegradable flocculating agents prepared by phosphate modification of Konjac. *Carbohydrate Polymer*. 67(4): 566-571.